Postprint of: Koziel S., Pietrenko-Dabrowska A., Al-Hasan M., Frequency-Based Regularization for Improved Reliability Optimization of Antenna Structures, IEEE Transactions on Antennas and Propagation (2020), DOI: 10.1109/TAP.2020.3044664

Frequency-Based Regularization for Improved Reliability Optimization of Antenna Structures

Slawomir Koziel, *Senior Member*, *IEEE,* Anna Pietrenko-Dabrowska, *Member, IEEE*, and Muath Al-Hasan, *Senior Member, IEEE*

***Abstract*—The paper proposes a modified formulation of antenna parameter tuning problem. The main ingredient of the presented approach is a frequency-based regularization. It allows for smoothening the functional landscape of the assumed cost function, defined to encode the prescribed design specifications. The regularization is implemented as a special penalty term complementing the primary objective and enforcing the alignment of the antenna responses with the target operating frequency (or frequencies for multi-band antennas). The result is an improved reliability and reduced cost of the optimization process, both highly desirable from the point of view of the efficacy of EM-driven design procedures. Furthermore, regularization makes the use of local routines sufficient even in situations where global search is otherwise imperative (e.g., due to poor initial design). Our methodology is demonstrated using three microstrip antennas. The superior performance of the approach, both in terms of design reliability and in terms of the computational cost of the optimization process, is corroborated by comparisons with a conventional formulation.**

***Index Terms*— Antenna optimization, gradient-based search, frequency-based regularization, EM analysis, EM-driven design.**

I. Introduction

Ever-increasing performance requirements, the emergence of new application areas (5G [1], internet of things [2], medical imaging [3]), the need for implementing various functionalities (circular polarization [4], MIMO operation [5], pattern diversity [6]), as well as the constraints on physical dimensions, are among those factors that make the design of modern antennas a challenging endeavor. To conform to the industry and consumer demands, contemporary antenna structures become more and more complex [7], described by multiple parameters [8], and—for reliability reasons—have to be evaluated using full-wave electromagnetic (EM) simulation tools [9], [10]. The latter may become a serious bottleneck whenever massive evaluations are required. A representative example of such an expensive procedure is numerical optimization [11], [12], which is otherwise imperative to boost the antenna performance beyond what is possible using parameter sweeping or theoretical models. Other tasks, e.g., uncertainty quantification [13], [14], or global optimization [15]-[17], entail even higher expenses.

Manuscript submitted on July ??, 2020. This work was supported in part by the Icelandic Centre for Research (RANNIS) Grant 206606051, by the National Science Centre of Poland Grant 2018/31/B/ST7/02369, and by the Abu-Dhabi Department of Education and Knowledge (ADEK) Award for Research Excellence 2019 under Grant AARE19-245.

S. Koziel is with Engineering Optimization and Modeling Center of Reykjavik University, Reykjavik, Iceland (e-mail: koziel@ru.is); A. Pietrenko-Dabrowska and also S. Koziel are with Faculty of Electronics, Telecommunications and Informatics, Gdansk University of Technology, 80-233 Gdansk, Poland. M. Al-Hasan is with the Networks and Communication Engineering Department, Al Ain University, Abu Dhabi, United Arab Emirates.

Expediting EM-driven optimization has been an important research topic, leading to numerous techniques that include adjoint sensitivities [18], [19], gradient-based procedures with sparse sensitivity updates [20], [21], surrogate-assisted algorithms employing both the approximation [22]-[24] and physics-based models [25]-[27] with a notable example of space mapping [28]. Data-driven metamodels and machine learning methods [29] are popular solutions for globalized search (e.g., efficient global optimization [30]). Yet another possibility is utilization of variable-fidelity EM simulations [31] along with the appropriate correction techniques (e.g., [32]). All of these methods have certain advantages but also drawbacks. In particular, surrogate-based procedures are very much limited by the problem dimensionality (data-driven models) [33], or are difficult to automate and require dedicated low-fidelity representations (physics-based models) [34].

Regardless of a particular optimization task, whether it is design closure [35], dimension scaling for a different operating frequency or substrate [36], or global search conducted to find a better parameter set of a topologically complex antenna, one of the most important issues is an appropriate allocation of the operating band(s) of the structure. From numerical optimization perspective, frequency-wise manipulation of the antenna characteristics is considerably more difficult than the level adjustment, especially for narrow- and multi-band antennas. This difficulty renders the application of local routines (e.g., gradient-based [37]) unreliable and computationally inefficient in many real-world cases.

This paper proposes a simple frequency-based regularization technique that allows us to mitigate the aforementioned problems and to improve the efficiency of the optimization process in a significant manner. The regularization is implemented through a reformulation of the cost function pertinent to the design task at hand by adding a penalty term that enforces the alignment of antenna characteristics with the target operating frequency (or frequencies). This does not only smoothen the functional landscape to be handled by the optimization algorithm and may reduce the cost of the parameter adjustment process, but also makes the use of local routines sufficient in cases where handling the task according to the original formulation would call for global search. The operation and performance of our methodology is illustrated using three examples of planar antennas. Benchmarking against conventional optimization is provided as well to demonstrate the advantages of the presented approach.

The novelty and the technical contributions of the work include: (i) the development of a frequency-based regularization scheme that enables efficient alignment of the antenna operating frequency (or frequencies) with their target values, (ii) reformulation of the objective function and the design optimization task that incorporates regularization and improves of the efficacy of the antenna parameter tuning process over conventional formulation (to the extent of addressing the issue of objective function multi-modality), (iii) the development of the versatile optimization framework demonstrated for various design scenarios (matching improvement, gain maximization, footprint reduction). To the best knowledge of the authors, none of these have been shown so far in the literature.

This article has been accepted for publication in a future issue of this journal, but has not been fully edited. Content may change prior to final publication. Citation information: DOI 10.1109/TAP.2020.3044664, IEEE Transactions on Antennas and Propagation

II. Optimization By Frequency-Based Regularization

This section outlines the proposed frequency-based regularization technique and places it in the context of antenna design closure using local optimization, here, trust-region gradient search. The latter is used to illustrate the regularization scheme, and can be replaced by other algorithms of choice in practical setups.

A. Optimization Problem Formulation

The following notation will be used throughout the paper. We denote by $\boldsymbol{R}(\boldsymbol{x})$ the response of the EM-simulated antenna model, where $\boldsymbol{x}$ is a vector of independent adjustable parameters (typically, antenna dimensions). To quantify the antenna performance, we use a scalar merit function $U(\boldsymbol{R}(\boldsymbol{x}))$, which is defined so that a better design corresponds to a lower value of U. The design problem is a nonlinear minimization task of the form

$$\boldsymbol{x}^* = \arg\min_{\boldsymbol{x}} U(\boldsymbol{R}(\boldsymbol{x})) \tag{1}$$

where $\boldsymbol{x}^*$ is the optimum design to be found. The analytical form of the merit function depends on the problem and the assumed treatment of the design constraints [25].

An example follows. Consider a multi-band antenna to be matched at the target operating frequencies $f_{0.K}$, k = 1, …, N. The minimax merit function is then defined as

$$U(\boldsymbol{R}(\boldsymbol{x})) = \max\{|S_{11}(\boldsymbol{x}, f_{0.1})|,\ldots,|S_{11}(\boldsymbol{x}, f_{0.N})|\} \tag{2}$$

where $S_{11}(\boldsymbol{x},f_{0.k})$ is antenna reflection at the design $\boldsymbol{x}$ and frequency f. As another example, consider an antenna that is to operate within the frequency range defined by its center frequency f_0 and the fractional bandwidth B, so that $|S_{11}| \le -10$ dB and the realized gain is to be maximized within at f_0. A possible formulation of the objective function (with implicit constraint handling) is

$$U(\boldsymbol{R}(\boldsymbol{x})) = -G(\boldsymbol{x}, f_0) + \beta c(\boldsymbol{x})^2 \tag{3}$$

Here, $G(\boldsymbol{x},f)$ is the realized gain at the frequency f, whereas $\beta c(\boldsymbol{x})$ is a penalty term (with β being a penalty coefficient) introduced to enforce $|S_{11}| \le -10$ dB over the bandwidth B. The penalty function may be defined to quantify a relative violation of the matching condition, e.g., $c(\boldsymbol{x})$ = $\max\{\max\{f_0(1 - B/2) \le f \le f_0(1 + B/2) : |S_{11}(\boldsymbol{x},f)| + 10\},0\}$.

B. Frequency-Based Regularization

As mentioned in the introduction, moving the antenna resonances to the intended frequencies is one of the challenging aspects of numerical optimization. This is illustrated in Fig. 1, showing the reflection and realized gain characteristics of a quasi-Yagi antenna considered in Section II. Re-designing the antenna for the target operating frequency of 5 GHz, and starting from the exemplary initial design shown in the picture, requires global search. This is because the initial design and the optimum are separated by a local maximum. Although the picture is a simplified representation of the problem (the initial and the optimum design are connected through a line segment), it gives a flavor of the practical challenges one may face when trying to apply numerical optimization.

To address this issue, we define a regularization function $f_r(\boldsymbol{x})$, which accounts for the discrepancies between the actual operating frequency (or frequencies) of the antenna and the target ones. The frequency-regularized objective function is then defined as

$$U_r(\boldsymbol{R}(\boldsymbol{x})) = U(\boldsymbol{R}(\boldsymbol{x})) + \beta_r \left[\max\left\{\frac{f_r(\boldsymbol{x}) - f_{r.\max}}{f_{r.\max}}, 0\right\}\right]^2 \tag{4}$$

where $f_{r.\max}$ is the maximum acceptable discrepancy between the actual and target operating frequency (or frequencies). The regularized objective function is defined to increase the original objective by the amount proportional (with the user-defined proportionality factor β_r) to the discrepancy quantified by f_r. However, the said contribution is zero if the discrepancy is sufficiently small (i.e., smaller than $f_{r.\max}$, also user-defined). This is to ensure that the original objective function is not distorted when the design approaches the optimum, and that the location of the optimum is the same w.r.t. to both U and U_r, assuming of course that the design for which $f_r(\boldsymbol{x}) \le f_{r.\max}$ is attainable. Furthermore, the regularization factor is smooth (continuously differentiable) with respect to f_r, which makes it appropriate to work with gradient-based optimization routines.

The effect of regularization is shown in Fig. 1(b): the functional landscape of the objective function is dramatically changed, and the reformulated problem becomes unimodal with the initial design being in the region of attraction of the optimum. Further, the optimum design according to the original objective function coincides with that of the regularized objective.

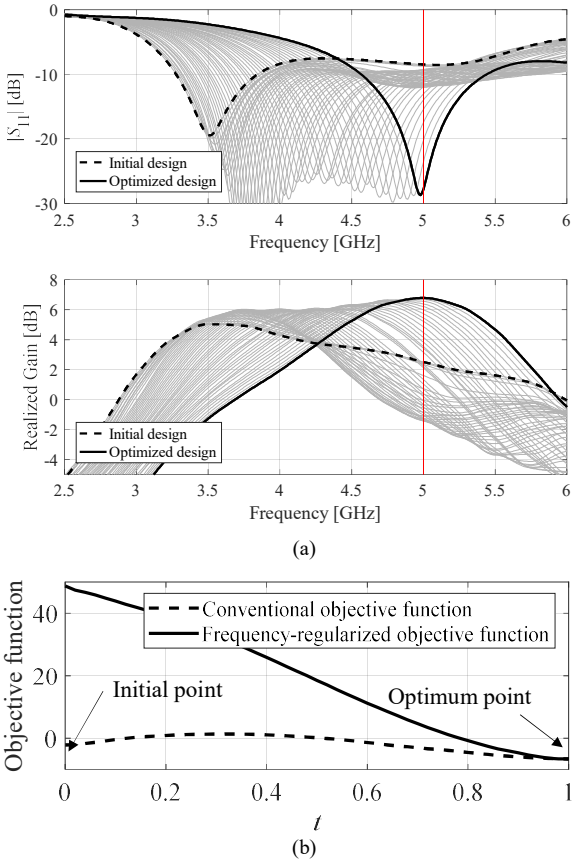

Fig. 1. Conceptual illustration of frequency-based regularization: (a) exemplary initial design for a quasi-Yagi antenna of Section III (thick dashed line), design optimized for the target frequency 5.0 GHz (thick solid line), and the family of antenna characteristics (reflection – top, realized gain – bottom) along the line segment connecting these two designs parameterized by $0 \le t \le 1$ (grey lines); (b) conventional objective function (3) (- - -) and frequency-regularized objective function (4) with the regularization function (5) (—) versus parameter t. It can be observed that the regularized objective function is monotonic, and the optimum design is attainable from the given initial point using local search routine, which is not the case for the conventional formulation.

This article has been accepted for publication in a future issue of this journal, but has not been fully edited. Content may change prior to final publication. Citation information: DOI 10.1109/TAP.2020.3044664, IEEE Transactions on Antennas and Propagation

A specific definition of a regularization function depends on a considered antenna structure and the type of response. For the quasi-Yagi antenna considered in Fig. 1, and optimized using the objective function (3), the regularization function can be defined as

$$f_r(\boldsymbol{x}) = \left| f_0 - \frac{f_{L.1} + f_{L.0} + f_{L.2}}{3} \right| \tag{5}$$

where $f_{L.j}$, j = 1, 2, are the frequencies corresponding to –10 dB levels of $|S_{11}|$, and $f_{L.0}$ is the frequency of the antenna resonance. If, at a particular design $\boldsymbol{x}$, the resonance level is above –10 dB, we assign $f_{L.j} = f_{L.0}$. In other words, the function f_r measures the distance between the target operating frequency and the approximate allocation of the antenna bandwidth (the average of the three frequencies mentioned above).

For the multi-band antenna optimized according to the minimax objective function (2), the regularization function can be defined as

$$f_r(\boldsymbol{x}) = \left\| \left[f_{0.1} \ldots f_{0.N} \right]^T - \left[f_1(\boldsymbol{x}) \ldots f_N(\boldsymbol{x}) \right]^T \right\| \tag{6}$$

where f_k, k = 1, …, N, are the actual resonant frequencies at the design $\boldsymbol{x}$, extracted from the EM simulation results.

C. Optimization Algorithm

The problem (1) can be solved using any available routine. Here, we use a trust-region gradient search [37]. The optimum $\boldsymbol{x}^*$ is approached through a series $\boldsymbol{x}^{(i)}$, i = 0, 1, …, produced as

$$\boldsymbol{x}^{(i+1)} = \arg \min_{\boldsymbol{x};\, -\boldsymbol{d}^{(i)} \le \boldsymbol{x} - \boldsymbol{x}^{(i)} \le \boldsymbol{d}^{(i)}} U(\boldsymbol{L}^{(i)}(\boldsymbol{x})) \tag{7}$$

in which $\boldsymbol{L}^{(i)}(\boldsymbol{x}) = \boldsymbol{R}(\boldsymbol{x}^{(i)}) + \boldsymbol{J}_{\boldsymbol{R}}^{(i)} \cdot (\boldsymbol{x} - \boldsymbol{x}^{(i)})$. The Jacobian $\boldsymbol{J}_{\boldsymbol{R}}$ is estimated using finite differentiation. The size vector $\boldsymbol{d}^{(i)}$ of the trust region is adjusted after each iteration using the standard rules [37]. Accelerated versions of (7), e.g., using sparse sensitivity updates are available [20], [21]; however, in this work, we focus on demonstrating the benefits of frequency-based regularization with little emphasis on reducing the cost of the optimization process by the algorithmic means.

III. Verification Case Studies

This section demonstrates the operation of the frequency-based regularization using three examples of planar antennas, each exhibiting different characteristics. We compare the efficacy of the optimization process involving the conventional formulation of the objective function and the regularized one in terms of the ability to find the satisfactory design but also the computational cost of the algorithm.

A. Quasi-Yagi Planar Antenna

The first example is a quasi-Yagi antenna with a parabolic reflector shown in Fig. 2 [38], implemented on FR4 substrate (ε_r = 4.4, h = 1.5 mm). The design variables are $\boldsymbol{x} = [W\ L\ L_m\ L_p\ S_d\ S_r\ W_2\ W_a\ W_d\ g]^T$ (all dimensions in mm). The computational model is implemented in CST Microwave Studio.

The design task is to optimize the antenna for a given center frequency f_0 while ensuring at least 8-percent impedance bandwidth (symmetric w.r.t. f_0). Furthermore, the realized gain is to be maximized at f_0. The conventional formulation of the optimization problem uses the objective function (3). The frequency-based regularization employs the regularization function (5) with $f_{r.\max}$ = 0.15 GHz. The antenna was optimized for f_0 = 2.5 GHz, f_0 = 4.5 GHz, and f_0 = 5.0 GHz, in all cases starting from the initial design that corresponds to the antenna operating at the frequency around 3.5 GHz. Figure 3 shows the initial and the optimized designs obtained using the standard and regularized formulations. It can be observed that the algorithm using the standard formulation was unable to find high-quality designs in neither of the considered cases, whereas applying regularization ensures reaching satisfactory design for all scenarios. The performance comparison has been provided in Table I. Thus, regularization allows for consistently yielding satisfactory design but also, the average optimization cost is lower than for the standard formulation (assuming the same termination criteria, which was 10^{-2} for the convergence in argument and 10^{-2} for for the trust region size).

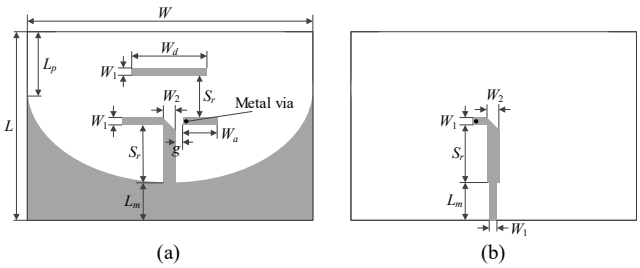

Fig. 2. Quasi-Yagi antenna with a parabolic reflector [38]: (a) top layer, (b) bottom layer.

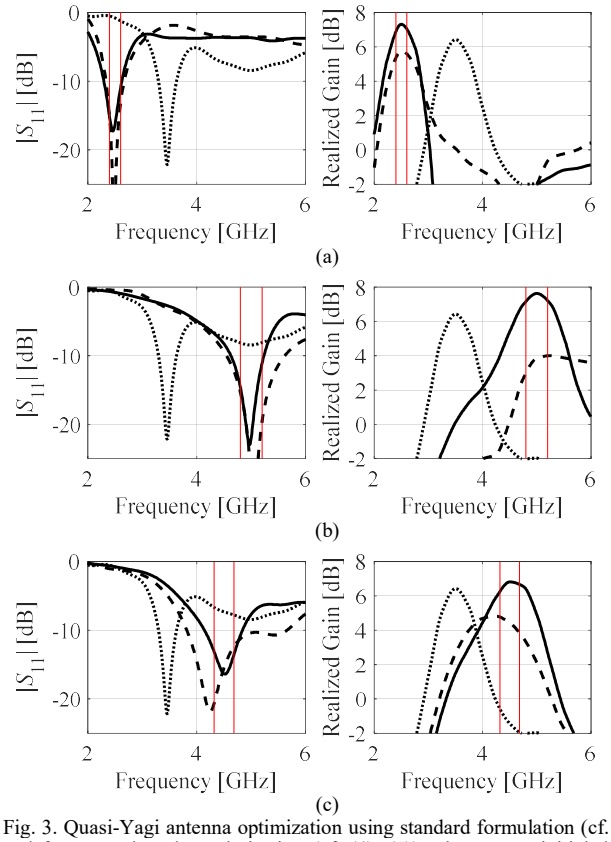

Fig. 3. Quasi-Yagi antenna optimization using standard formulation (cf. (3)), and frequency-based regularization (cf. (4), (5)). Shown are: initial design (····), optimum found using standard formulation (- - -), optimum found with regularization (—). Target frequencies: (a) 2.5 GHz, (b) 4.5 GHz, (c) 5.0 GHz. Vertical lines mark the intended operating bandwidth of the antenna.

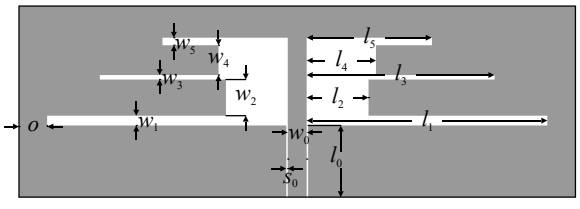

Fig. 4. Geometry of the triple-band dipole antenna.

B. Triple-Band Dipole Antenna

The second example is a triple-band uniplanar dipole antenna shown in Fig. 4 [39], implemented on RO4350 substrate. The adjustable parameters are $\boldsymbol{x} = [l_1\ l_2\ l_3\ l_4\ l_5\ w_1\ w_2\ w_3\ w_4\ w_5]^T$; other parameters are fixed: $l_0 = 30$, $w_0 = 3$, $s_0 = 0.15$ and $o = 5$ (all dimensions in mm). As before, the computational model is implemented in CST. The task is to improve antenna matching at the operating frequencies $f_{0.1} = 2.45$ GHz, $f_{0.2} = 3.6$ GHz, and $f_{0.3} = 5.3$ GHz. The standard (minimax) formulation employs the objective function (2). The frequency-based regularization uses the regularization function (6) with $f_{r.\max} = 0.15$ GHz.

The antenna was optimized using three different starting points. The reflection responses at the designs found using both approaches are shown in Fig. 5. The optimization procedure using the minimax formulation was only able to find a (more or less) satisfactory design for one of the initial designs, whereas the formulation incorporating regularization was successful in all cases. The performance differences between formulations are consistent with the previous example (cf. Table II): the design quality is significantly better, whereas the computational cost is lower when using regularization.

C. Compact Ultra-wideband Monopole Antenna

The last example is the ultra-wideband monopole [40], implemented on RF-35 substrate ($\varepsilon_r = 3.5$, $h = 0.762$ mm), shown in Fig. 6. The adjustable parameters are $\boldsymbol{x} = [L_0\ dR\ R\ r_{rel}\ dL\ dw\ L_g\ L_1\ R_1\ dr\ c_{rel}]^T$. The EM model is implemented in CST, and incorporates the SMA connector. The operating frequency range of the antenna is 3.1 GHz to 10.6 GHz. The design objective is to minimize the antenna footprint $A(\boldsymbol{x})$ while ensuring that $|S_{11}(\boldsymbol{x},f)| \le -10$ dB within the operating band.

The objective function is defined as

$$U(\boldsymbol{R}(\boldsymbol{x})) = A(\boldsymbol{x}) + \beta c(\boldsymbol{x})^2 \tag{8}$$

where the penalty function takes the form $c(\boldsymbol{x}) = \max\{\max\{3.1\text{ GHz} \le f \le 10.6\text{ GHz} : |S_{11}(\boldsymbol{x},f)| + 10\},0\}$. The regularization function is defined as

$$f_r(\boldsymbol{x}) = \left| f_L - f_{r.1} \right| \tag{9}$$

where $f_L = 3.1$ GHz and $f_{r.1}$ is the lowest frequency corresponding to –10 dB level of reflection (or the frequency of the first antenna resonance if the resonance level is above –10 dB). The reason for this setup is that the minimum-size design is normally such that the matching condition is barely met (or slightly violated when using implicit constraint handling as in (8) [41]), with the first antenna resonance close to the lower edge of the operating band (here, 3.1 GHz). By enforcing this resonance to be close to that frequency, the problem of reducing the antenna size becomes numerically more tractable.

For the sake of demonstration, we optimize the antenna using three different starting points, as illustrated in Fig. 7. Regularization (4), (9) leads to considerably better results than the standard formulation (8), cf. Table III. In all cases, the condition $|S_{11}(\boldsymbol{x},f)| \le -10$ dB is satisfied in a satisfactory manner, but the obtained footprint area is smaller for the algorithm using regularization. It should be emphasized that optimization-based size reduction is a challenging problem from the numerical perspective because the reflection constraint is active at the optimum. Locating it requires traversing the boundary of the feasible region, and the results are typically dependent on the starting point, partially due to numerical noise issues.

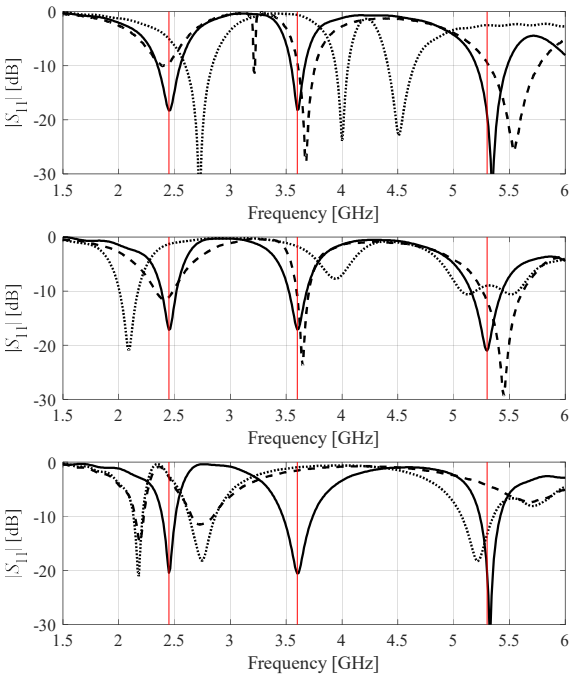

Fig. 5. Triple-band antenna optimization using standard formulation (cf. (2)), and frequency-based regularization (cf. (4), (6)). Shown are: initial design (····), optimum found using standard formulation (- - -), optimum found with regularization (—) for three different initial designs. Target frequencies are 2.45 GHz, 3.6 GHz, and 5.3 GHz.

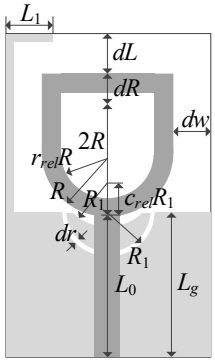

Fig. 6. Geometry of the ultra-wideband monopole antenna [40]. The ground plane marked using the light gray shade.

TABLE I QUASI-YAGI ANTENNA: OPTIMIZATION PERFORMANCE

Problem formulation	Target frequency	Results			
		Individual Case		Average	
		Cost[#]	$U(\boldsymbol{R}(\boldsymbol{x}))$[$]	Cost[#]	$U(\boldsymbol{R}(\boldsymbol{x}))$[$]
Standard (cf. (3))	2.5 GHz	165	–5.7 dB	171	–4.6 dB
	4.5 GHz	123	–3.7 dB		
	5.0 GHz	224	–4.4 dB		
Regularization (this work, cf. (4), (5))	2.5 GHz	147	–7.2 dB	131	–7.1 dB
	4.5 GHz	135	–7.5 dB		
	5.0 GHz	110	–6.7 dB		

[#] Cost expressed in the number of EM simulations of the antenna.
[$] Objective function value according to the function (3).

TABLE II TRIPLE-BAND ANTENNA: OPTIMIZATION PERFORMANCE

Problem formulation	Initial Design	Results			
		Individual Case		Average	
		Cost[#]	$U(\boldsymbol{R}(\boldsymbol{x}))$[$]	Cost[#]	$U(\boldsymbol{R}(\boldsymbol{x}))$[$]
Standard (cf. (3))	1	247	–9.4 dB	157	–7.4 dB
	2	108	–11.1 dB		
	3	115	–1.5 dB		
Regularization (this work, cf. (4), (5))	1	183	–18.2 dB	144	–18.6 dB
	2	113	–17.7 dB		
	3	135	–20.5 dB		

[#] Cost expressed in the number of EM simulations of the antenna.
[$] Objective function value according to the function (2).

TABLE III UWB ANTENNA: OPTIMIZATION PERFORMANCE

Problem formulation	Initial Design	Results			
		Individual Case		Average	
		Cost[#]	Area[$]	Cost[#]	Area[$]
Standard (cf. (8))	1	93	261 mm^2	113	293 mm^2
	2	101	401 mm^2		
	3	146	216 mm^2		
Regularization (this work, cf. (4), (9))	1	125	238 mm^2	138	219 mm^2
	2	151	201 mm^2		
	3	138	219 mm^2		

[#] Cost expressed in the number of EM simulations of the antenna.
[$] Footprint area of the optimized antenna.

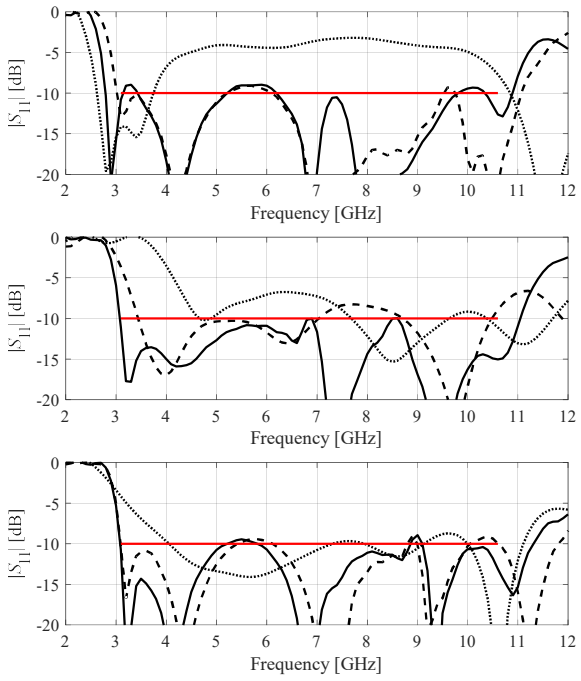

Fig. 7. Ultra-wideband monopole antenna optimization using standard formulation (cf. (8)), and frequency-based regularization (cf. (4), (9)). Shown are: initial design (····), optimum found using standard formulation (- - -), optimum found with regularization (—) for three different initial designs. Target operating band 3.1 GHz to 10.6 GHz is marked using the horizontal line.

Notwithstanding, regularization noticeably improves repeatability of the results compared to the standard formulation because it allows for quick adjustment of the lower edge of the operating bandwidth, which yields a better position before further tuning. At the same time, the optimization cost with regularization is slightly higher as the algorithm using the standard formulation often converges prematurely.

IV. CONCLUSION

This communication proposed a frequency-based regularization approach for reliable parameter tuning of antennas. It is incorporated into the objective function through a penalty term that quantifies the discrepancy between the target and the actual operating conditions of the antenna in terms of the relevant frequencies (e.g., allocation of the antenna resonances). The regularization function is formulated to be smooth (i.e., continuously differentiable) and only contributes to the primary objective if the aforementioned discrepancies are beyond the acceptance limit decided by the user. It has an effect of smoothing out the functional landscape to be optimized, and mitigates the multi-modality issues, but it does not modify the original objective when close to the optimum.

Our methodology has been validated using three planar structures, optimized under different scenarios (matching improvement, gain maximization, size reduction). A significant improvement of the search process efficacy has been demonstrated over the conventional design closure task formulations. This includes reducing the sensitivity of the optimization outcome to the initial design, a possibility of re-designing antenna structures for the operating frequencies significantly different from those at the starting point, as well as improving repeatability of solutions. An additional benefit resulting from regularization-based problem reformulation is that local methods may be sufficient in the cases that otherwise require global search. In other words, regularization may alleviate the difficulties pertinent to a possible presence of multiple local minima of the standard objective functions. Overall, the presented approach can be a useful algorithmic tool for handling problems where the standard setup (e.g., a minimax objective function) is prone to a failure. It may also alleviate the difficulties originating from poor initial designs.

ACKNOWLEDGMENT

The authors would like to thank Dassault Systemes, France, for making CST Microwave Studio available.

REFERENCES

[1] Z. Nie, H. Zhai, L. Liu, J. Li, D. Hu, and J. Shi, "A dual-polarized frequency-reconfigurable low-profile antenna with harmonic suppression for 5G application," *IEEE Ant. Wireless Prop. Lett.*, vol. 18, no. 6, pp. 1228-1232, 2019.

[2] Y. Wang, J. Zhang, F. Peng, and S. Wu, "A glasses frame antenna for the applications in internet of things," *IEEE Internet of Things J.*, vol. 6, no. 5, pp. 8911-8918, 2019.

[3] M. Rokunuzzaman, M. Samsuzzaman, and M.T. Islam, "Unidirectional wideband 3-D antenna for human head-imaging application," *IEEE Ant. Wireless Prop. Lett.*, vol. 16, pp. 169-172, 2017.

[4] P. Kumar, S. Dwari, R.K. Saini, and M.K. Mandal, "Dual-band dual-sense polarization reconfigurable circularly polarized antenna," *IEEE Ant. Wireless Prop. Lett.*, vol. 18, no. 1, pp. 64-68, 2019.

[5] Y. Liu, Z. Ai, G. Liu, and Y. Jia, "An integrated shark-fin antenna for MIMO-LTE, FM, and GPS applications," *IEEE Ant. Wireless Prop. Lett.*, vol. 18, no. 8, pp. 1666-1670, 2019.

[6] Y. Dong, J. Choi, and T. Itoh, "Vivaldi antenna with pattern diversity for 0.7 to 2.7 GHz cellular band applications," *IEEE Ant. Wireless Prop.*

Lett., vol. 17, no. 2, pp. 247-250, 2018.

[7] Y. Cui, C. Qi, and R. Li, "A low-profile broadband quad-polarization reconfigurable omnidirectional antenna," *IEEE Trans. Ant. Prop.*, vol. 67, no. 6, pp. 4178-4183, 2019.

[8] Y. Cui, P. Luo, Q. Gong, and R.L. Li, "A compact tri-band horizonally polarized omnidirectional antenna for UAV applications," *IEEE Ant. Wireless Prop. Lett.*, vol. 18, no. 4, pp. 601-605, 2019.

[9] K.Y. Kapusuz, S. Lemey, A. Petrocchi, P. Demeester, D. Schreurs, and H. Rogier, "Polarization reconfigurable air-filled substrate integrated waveguide cavity-backed slot antenna," *IEEE Access*, vol. 7, pp. 102628-102643, 2019.

[10] L. Sun, Y. Li, Z. Zhang, and Z. Feng, "Compact co-horizontally polarized full-duplex antenna with omnidirectional patterns," *IEEE Ant. Wireless Prop. Lett.*, vol. 18, no. 6, pp. 1154-1158, 2019.

[11] X.S. Yang, J. Wang, and B.Z. Wang, "Topology optimization of patch antennas with specified polarization and beam characteristics," *In 6th Asia-Pacific Conf. Ant. Propag.*, Xian, China, Oct. 2017.

[12] R. Lehmensiek and D. de Villiers, "Optimization of log-periodic dipole array antennas for wideband omnidirectional radiation," *IEEE Trans. Ant. Propag.*, vol. 63, no. 8, pp. 3714-3718, 2015.

[13] I. Syrytsin, S. Zhang, G.F. Pedersen, K. Zhao, T. Bolin, and Z. Ying, "Statistical investigation of the user effects on mobile terminal antennas for 5G applications," *IEEE Trans. Ant. Prop.*, vol. 65, no. 12, pp. 6596-6605, 2017.

[14] L. Cai, Y. Zhao, W. Chen, P. Huang, X. Liu, and X. Zhang, "Self-heating aware EM reliability prediction of advanced CMOS technology by kinetic Monte Carlo method," *Int. Symp. Physical and Failure Anal. Int. Circuits*, Hangzhou, China, July 2-5, 2019.

[15] A.A. Al-Azza, A.A. Al-Jodah, and F.J. Harackiewicz, "Spide monkey optimization: a novel technique for antenna optimization," *IEEE Ant. Wireless Prop. Lett.*, vol. 15, pp. 1016-1019, 2016.

[16] M. Tang, X. Chen, M. Li, R. W. Ziolkowski, "Particle swarm optimized, 3-D-printed, wideband, compact hemispherical antenna," *IEEE Ant. Wireless Propag. Lett.*, vol. 17, no. 11, pp. 2031-2035, 2018.

[17] M. Li, Y. Liu, and Y.J. Guo, "Shaped power pattern synthesis of a linear dipole array by element rotation and phase optimization using dynamic differential evolution," *IEEE Ant. Wireless Prop. Lett.*, vol. 17, no. 4, pp. 697-701, 2018.

[18] S. Koziel, F. Mosler, S. Reitzinger, and P. Thoma, "Robust microwave design optimization using adjoint sensitivity and trust regions," *Int. J. RF and Microwave CAE*, vol. 22, no. 1, pp. 10-19, 2012.

[19] J. Wang, X.S. Yang, and B.Z. Wang, "Efficient gradient-based optimisation of pixel antenna with large-scale connections," *IET Microwaves Ant. Prop.*, vol. 12, no. 3, pp. 385-389, 2018.

[20] A. Pietrenko-Dabrowska and S. Koziel, „Computationally-efficient design optimization of antennas by accelerated gradient search with sensitivity and design change monitoring," *IET Microwaves Ant. Prop.*, vol. 14, no. 2, pp. 165-170, 2020.

[21] S. Koziel and A. Pietrenko-Dabrowska, "Expedited optimization of antenna input characteristics with adaptive Broyden updates," *Eng. Comp.*, vol. 37, no. 3, 2019.

[22] D.I.L. de Villiers, I. Couckuyt, and T. Dhaene, "Multi-objective optimization of reflector antennas using kriging and probability of improvement," *Int. Symp. Ant. Prop.*, pp. 985-986, San Diego, USA, 2017.

[23] J.P. Jacobs, "Characterisation by Gaussian processes of finite substrate size effects on gain patterns of microstrip antennas," *IET Microwaves Ant. Prop.*, vol. 10, no. 11, pp. 1189-1195, 2016.

[24] A.K. Hassan, A.S. Etman, and E.A. Soliman, "Optimization of a novel nano antenna with two radiation modes using kriging surrogate models," *IEEE Photonics Journal*, vol. 10, no. 4, article no. 4800807, 2018.

[25] S. Koziel and S. Ogurtsov, *Simulation-based optimization of antenna arrays*, World Scientific, 2019.

[26] Y. Su, J. Lin, Z. Fan, and R. Chen, "Shaping optimization of double reflector antenna based on manifold mapping," *Int. Applied Computational Electromagnetic Society Symp. (ACES)*, pp. 1-2, 2017.

[27] S. Koziel and S.D. Unnsteinsson "Expedited design closure of antennas by means of trust-region-based adaptive response scaling," *IEEE Antennas Wireless Prop. Lett.*, vol. 17, no. 6, pp. 1099-1103, 2018.

[28] J. Xu, M. Li, and R. Chen, "Space mapping optimisation of 2D array elements arrangement to reduce the radar cross-scattering," *IET Microwaves Ant. Prop.*, vol. 11, no. 11, pp. 1578-1582, 2017.

[29] L.Y. Xiao, W. Shao, X. Ding, and B.Z. Wang, "Dynamic adjustment kernel extreme learning machine for microwave component design," *IEEE Trans. Microwave Theory Tech.*, vol. 66, no. 10, pp. 4452-4461, 2018.

[30] A.C. Berbecea, R. Ben-Ayed, F. Gillion, S. Brisset, and P. Brisset, "Comparison of efficient global optimization and output space mapping on the biobjective optimization of a safety isolating transformer," *IEEE Trans. Magn.*, vol. 48, no. 2, pp. 791-794, 2012.

[31] J. Gong, F. Gillon, J.T. Canh, and Y. Xu, "Proposal of a kriging output space mapping technique for electromagnetic design optimization," *IEEE Trans. Magn.*, vol. 53, no. 6, pp. 1-4, 2017.

[32] S. Koziel and L. Leifsson, *Simulation-driven design by knowledge-based response correction techniques*, Springer, New York, 2016.

[33] S. Koziel and A. Pietrenko-Dabrowska, *Performance-driven surrogate modeling of high-frequency structures*, Springer, New York, 2020.

[34] S. Koziel, J.W. Bandler, and K. Madsen, "Quality assessment of coarse models and surrogates for space mapping optimization," *Optimization and Engineering*, vol. 9, no. 4, pp. 375-391, 2008.

[35] J. Tak, A. Kantemur, Y. Sharma, and H. Xin, "A 3-D-printed W-band slotted waveguide array antenna optimized using machine learning," *IEEE Ant. Wireless Prop. Lett.*, vol. 17, no. 11, pp. 2008–2012, 2018.

[36] A. Pietrenko-Dabrowska and S. Koziel, „Accelerated design optimization of miniaturized microwave passives by design reusing and kriging interpolation surrogates," *AEU Int. J. Electronics Comm.*, vol. 118, 2020.

[37] A. R. Conn, N. I. M. Gould, and P. L. Toint, *Trust Region Methods*, Philadelphia, PA, USA: MPS-SIAM Series on Optimization, 2000.

[38] Z. Hua, G. Haichuan, L. Hongmei, L. Beijia, L. Guanjun, and W. Qun, "A novel high-gain quasi-Yagi antenna with a parabolic reflector," *Int. Symp. Ant. Prop. (ISAP)*, Hobart, Australia, 2015.

[39] Y.-C. Chen, S.-Y. Chen, and P. Hsu, "Dual-band slot dipole antenna fed by a coplanar waveguide," *IEEE Int. Symp. Ant. Prop.*, pp. 3589-3592, 2006.

[40] M. G. N. Alsath and M. Kanagasabai, "Compact UWB monopole antenna for automotive communications," *IEEE Trans. Ant. Prop.*, vol. 63, no. 9, pp. 4204–4208, 2015.

[41] D.O. Johanesson and S. Koziel, "Feasible space boundary search for improved optimization-based miniaturization of antenna structures," *IET Microwaves, Ant. Prop.*, vol. 12, no. 8, pp. 1273-1278, 2018.